Bridge helix of Cas12a imparts selectivity for *cis*-DNA cleavage and regulates *trans*-DNA cleavage

Hari Priya Parameshwaran[1], Kesavan Babu[1], Christine Tran[1], Kevin Guan[1,2], Aleique Allen[3], Venkatesan Kathiresan[3], Peter Z. Qin[3], Rakhi Rajan[1*]

Supporting information:

SI FIGURES

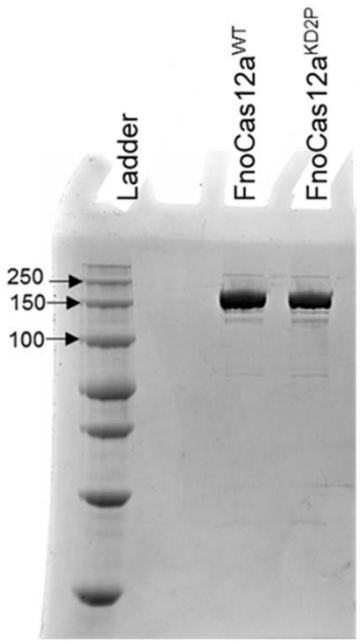

Fig. S1. Analysis of protein purity. A 10% SDS gel showing the purity of the FnoCas12a^{WT} and FnoCas12a^{KD2P} proteins after a three-step purification protocol. The protein ladder shows the protein to be the correct size at ~152 kDa.

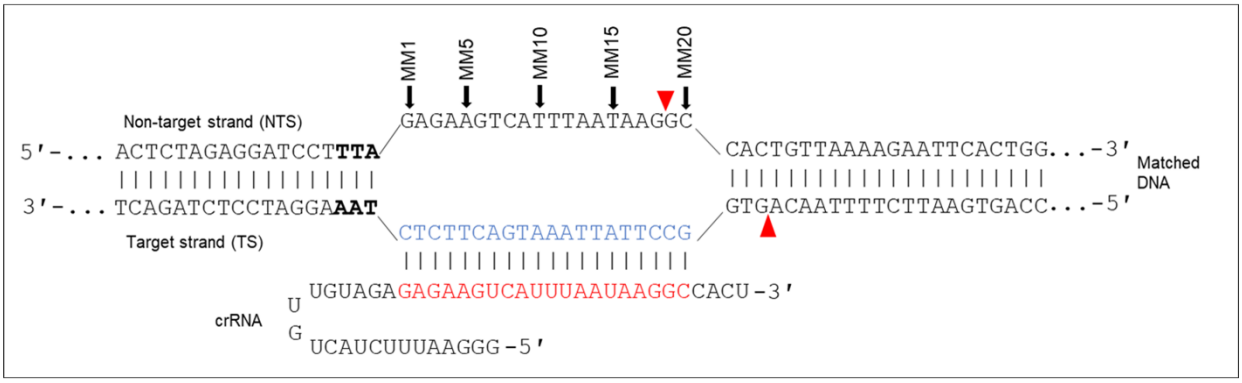

Fig. S2. Illustration of R-loop formation with matched DNA. The image shows the organization of R-loop formed by Cas12a. The PAM sequence is in bold. The sequence in red corresponds to the guide region of the crRNA that hybridizes with the target strand (TS, blue) of the DNA. The 5′ terminus of the crRNA forms the pseudoknot. A 3-nt addition (GGG) was introduced to the crRNA sequence at the 5′ terminus to increase the efficiency of *in vitro* transcription. The numbering scheme for mismatches is relative to position of PAM on the NTS and a few mismatch positions are labeled for clarity. The red arrows represent the cleavage sites on TS (23rd downstream of PAM) and NTS (18th downstream of PAM) of target DNA producing a staggered product after Cas12a cleavage.

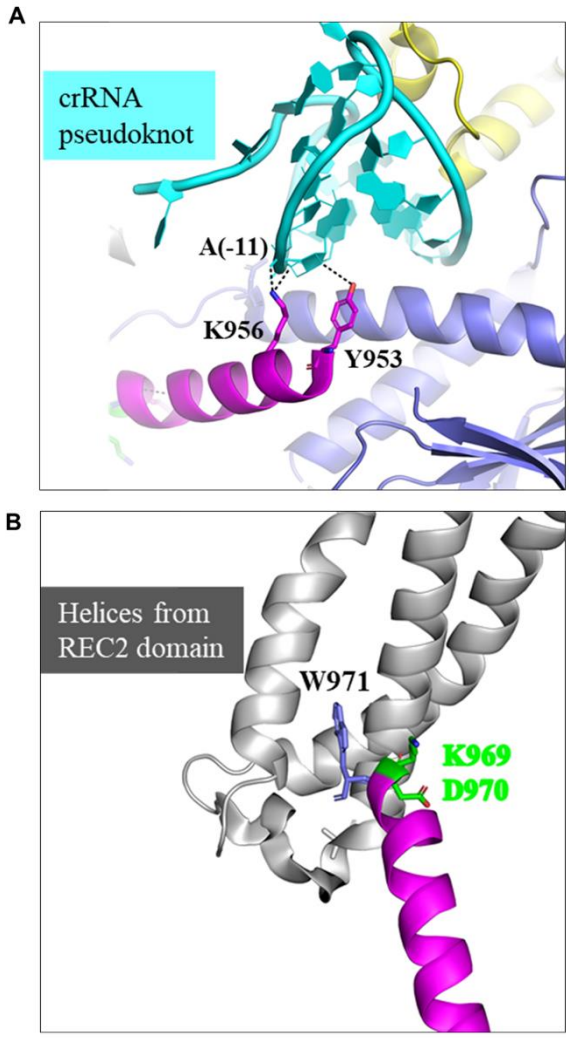

Fig S3. Interactions of BH with crRNA and REC2 domain. (A) A zoomed-in representation of the interactions of N-terminal BH residues with the pseudoknot region of the crRNA. Y953 interacts with A(-11), while K956 interacts with both C(-10) and A(-11) of the crRNA pseudoknot. Negative numbers of crRNA represents nt in the repeat region of crRNA, while nt in guide region are represented with positive numbers. **(B)** Figure representing the positioning of W971 with respect to the K969 and D970. The indole ring of W971 is wedged between two helices (comprising residues 523-587) of the REC2 domain.

Fig. S4: Analysis of one *vs.* two exponential fit for supercoiled plasmid cleavage data

Figure S4 shows one-exponential fit (eq. 10, main text) for the loss of supercoiled plasmid DNA precursor. To analyze the one-exponential vs. two-exponential fit, the two-exponential fit of loss of supercoiled plasmid DNA precursor (eq.11 in main text, designated as the "Full" model) was compared to the one-exponential fit (designated as the "Reduced" model). The error sum of the squares for the Full model (SSE(F)) and the reduced model (SSE(R)) were computed as:

$$SSE(F) = \sum_{i=0}^{12}[P_i(obs) - P_i(F)]^2 \quad (15)$$

$$SSE(R) = \sum_{i=0}^{12}[P_i(obs) - P_i(R)]^2 \quad (16)$$

where P_i(obs) represents the observed experimental value of the supercoiled precursor (i.e., Frac[P]) at a given time point, P_i(F) and P_i(R) represent, respectively, the corresponding values computed using parameters obtained from the Full and Reduced models.

The F* value was then computed according to:

$$F^*_{dF,dF(F)} = \frac{[SSE(R) - SSE(F)]/dF}{SSE(F)/dF(F)} \quad (17)$$

where dF(F) = 8 is the degree of freedom of the Full model (i.e., 12 data points and 4 fitting parameters), dF(R) = 10 is the degree of freedom of the Reduced model (i.e., 12 data points and 2 fitting parameters), and dF = dF(R) - dF(R) = 2. The *p* value was then obtained based on the F* using an ANOVA (Analysis of Variance) calculator.

The F-test yielded $F^*_{2,8}$ = 20.5 and $p = 7.1 \times 10^{-4}$ for the FnoCas12a^{WT} dataset and $F^*_{2,8}$ = 18.6 and $p = 9.8 \times 10^{-4}$ for the FnoCas12a^{KD2P} dataset. Since both *p* values are less than 0.01, the analyses indicate that with a Significance Level of 0.01, the Full model (i.e., two-exponential fit) can be accepted over the Reduced model (i.e., single-exponential fit). In addition, note that with the single-exponential fit, k_{obs} of FnoCas12a^{KD2P} (2.93 ± 0.36 min^{-1}) is 2.7 fold smaller than that of FnoCas12a^{WT} (7.90 ± 1.63 min^{-1}) (Figure S4). This is very similar to the 3-fold reduction of k_1 from the two-exponential fit (see Figure 2).

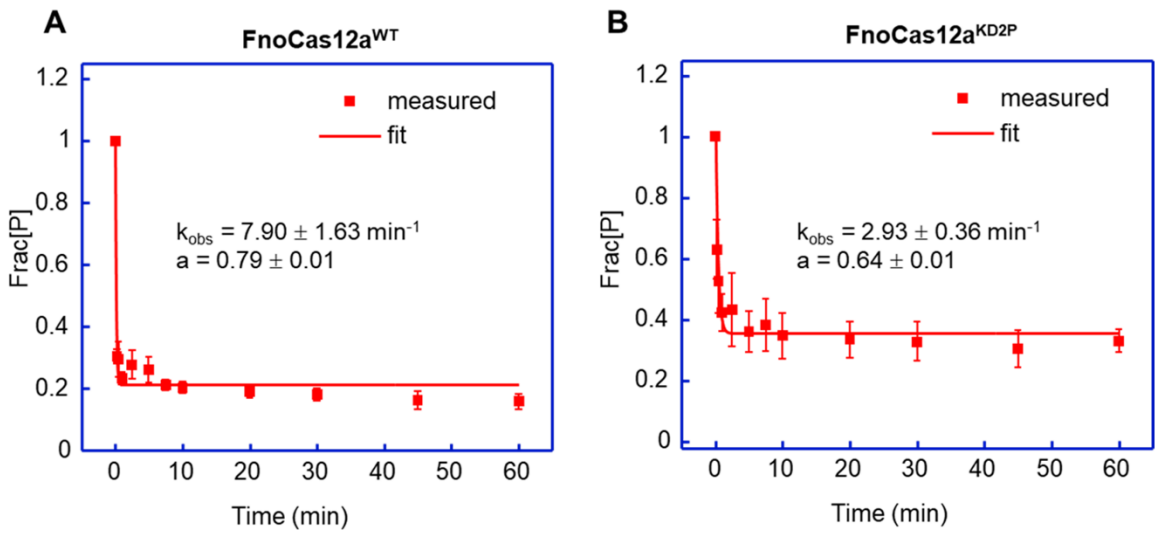

Fig. S4. Analysis of one *vs.* two exponential fit for supercoiled plasmid cleavage data. Our data shows that two-exponential fit for the loss of supercoiled plasmid DNA precursor was better suited than one-exponential. This figure shows fit from one-exponential model. In each panel the average fraction of precursor (Frac[P]) was plotted *vs.* time, with the error bars representing the SEM of different replications. The data were fit to a single-exponential decay, $Frac[P] = 1 - a \cdot [1 - \exp(-k_{obs} \cdot t)]$ (eq. 10, main text), with "k_{obs}" being the reaction rate constant and "a" being the total active fraction. **(A)** FnoCas12a^{WT} cleavage. The parameters obtained were k_{obs} = 7.90 ± 1.63 min^{-1} and a = 0.79 ± 0.01. **(B)** FnoCas12a^{KD2P} cleavage. The parameters obtained were k_{obs} = 2.93 ± 0.36 min^{-1} and a = 0.64 ± 0.01.

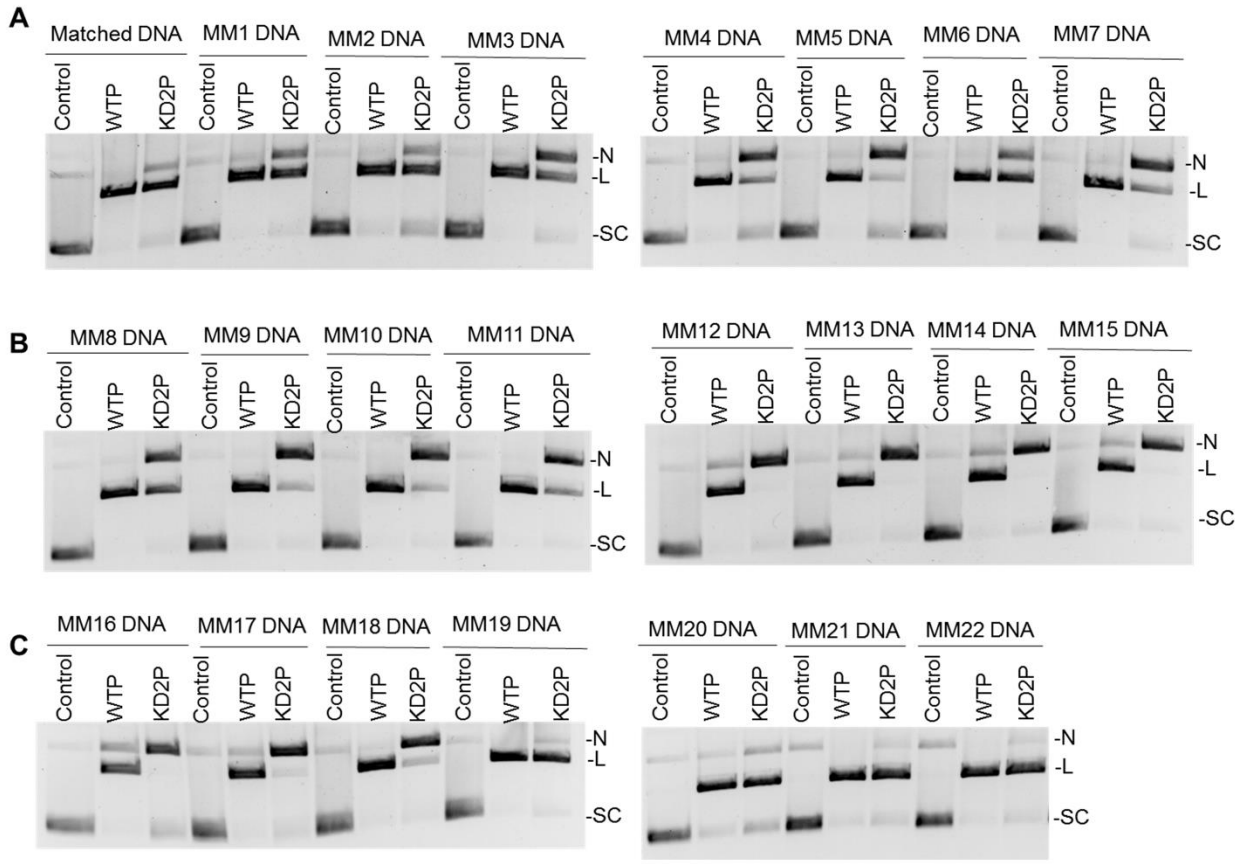

Fig. S5. Representative gel images comparing the activities of FnoCas12a^{WT} and FnoCas12a^{KD2P} on different mismatch-containing plasmid substrates. (A-C) 25 nM RNP was incubated with substrate for 15 min at 37°C. [N: nicked, L: linear, SC: supercoiled, WTP: FnoCas12a^{WT}, KD2P: FnoCas12a^{KD2P}, MM: mismatch and the number indicates the mismatch position on the NTS with respect to PAM]. A total of three replications were performed for each reaction.

A

FnoCas12a^{WT}

	Nicked (%)	Linear (%)	Total cleavage (%)
Matched DNA	-18 ± 7	90 ± 0	71 ± 7
MM1	-1 ± 1	82 ± 4	81 ± 5
MM2	-1 ± 2	79 ± 2	77 ± 4
MM3	-5 ± 5	89 ± 2	84 ± 6
MM4	-5 ± 3	74 ± 4	69 ± 7
MM5	2 ± 4	80 ± 3	81 ± 6
MM6	-8 ± 4	88 ± 2	80 ± 5
MM7	0 ± 2	83 ± 3	83 ± 5
MM8	-1± 3	90 ± 1	89 ± 4
MM9	2 ± 4	86 ± 2	88 ± 3
MM10	-12 ± 4	94 ± 2	82 ± 4
MM11	-7 ± 2	93 ± 1	86 ± 3
MM12	15 ± 4	69 ± 4	83 ± 3
MM13	12 ± 3	74 ± 3	86 ± 2
MM14	13 ± 1	71 ± 3	83 ± 2
MM15	8 ± 5	64 ± 5	72 ± 7
MM16	19 ± 1	66 ± 1	85 ± 2
MM17	3 ± 1	69 ± 5	72 ± 5
MM18	-6 ± 2	83 ± 2	77 ± 3
MM19	-15 ± 4	97 ± 0	82 ± 4
MM20	-13 ± 7	91 ± 4	78 ± 4
MM21	-4 ± 4	93 ± 1	89 ± 5
MM22	-11 ± 1	94 ± 1	83 ± 2

B

FnoCas12a^{KD2P}

	Nicked (%)	Linear (%)	Total cleavage (%)
Matched DNA	-4 ± 6	71 ± 3	67 ± 6
MM1	19 ± 3	60 ± 1	79 ± 3
MM2	13 ± 3	61 ± 2	73 ± 4
MM3	37 ± 6	43 ± 2	80 ± 5
MM4	33 ± 5	31 ± 3	65 ± 4
MM5	55 ± 4	18 ± 2	74 ± 3
MM6	21 ± 5	57 ± 2	78 ± 5
MM7	50 ± 4	29 ± 1	78 ± 4
MM8	43 ± 4	45 ± 1	88 ± 4
MM9	58 ± 8	29 ± 5	87 ± 2
MM10	53 ± 9	28 ± 4	81 ± 5
MM11	49 ± 5	34 ± 3	84 ± 2
MM12	74 ± 4	5 ± 1	79 ± 3
MM13	77 ± 2	3 ± 1	81 ± 2
MM14	75 ± 4	4 ± 1	79 ± 3
MM15	66 ± 9	3 ± 1	70 ± 8
MM16	61 ± 6	5 ± 1	66 ± 5
MM17	62 ± 3	7 ± 3	68 ± 6
MM18	53 ± 5	22 ± 3	75 ± 3
MM19	-4 ± 5	84 ± 3	79 ± 4
MM20	0 ± 4	71 ± 3	71 ± 3
MM21	8 ± 6	77 ± 4	85 ± 5
MM22	-1 ± 3	81 ± 3	81 ± 2

Fig. S6. Tables depicting the values of nicked, linear and total cleavage for (A) FnoCas12a^{WT} and (B) FnoCas12a^{KD2P}. The negative values for nicked DNA indicate that nicked population present in the substrate is being cleaved by FnoCas12a. Note that the presence of nicked band in the plasmid preparation tends to reduce the total activity compared to the amount of linear activity (example: see FnoCas12a^{WT} activity with matched DNA). Nevertheless, the table gives an indication of the total activity and ability of the proteins to linearize and nick different DNA substrates and can clearly relay the efficiency to cleave different mismatch positions and the role of BH in mismatch discrimination.

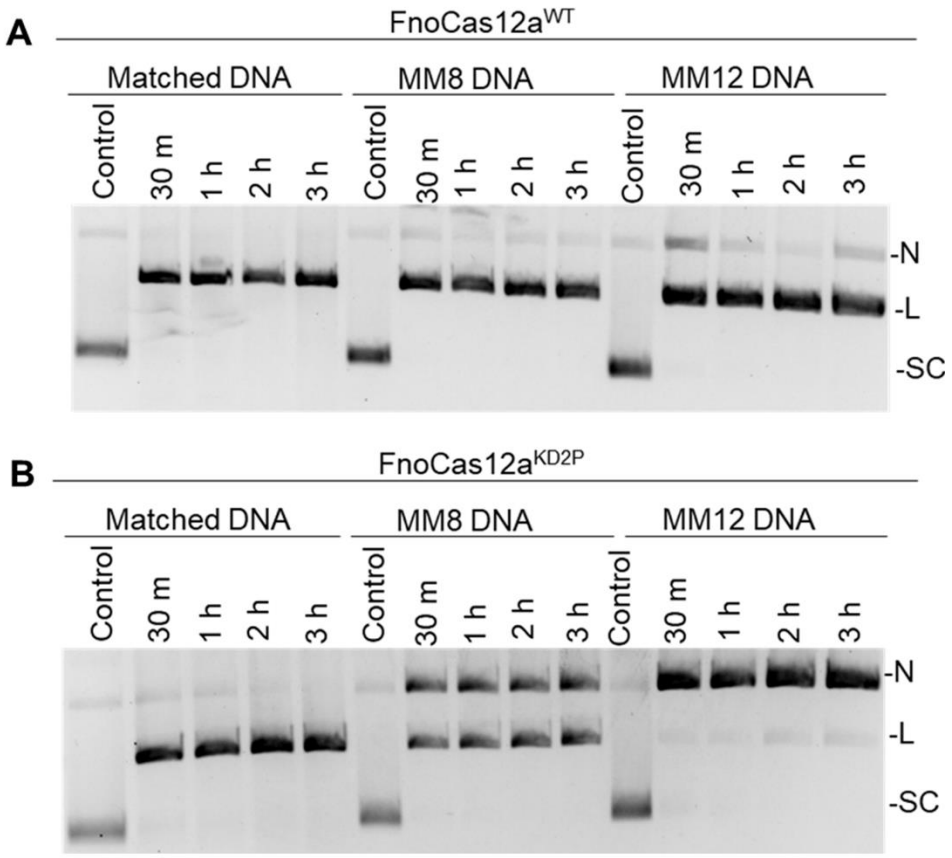

Fig. S7. Gels showing the effect of longer incubation times on cleavage of matched DNA, MM8 DNA and MM12 DNA by (A) FnoCas12a^{WT} and (B) FnoCas12a^{KD2P}. [N: nicked, L: linear, SC: supercoiled, MM: mismatch and the number indicates the mismatch position on the NTS with respect to PAM, m: min, h: hours]**.** Representative gels from two replications.

Fig. S8: Analysis of *cis*-cleavage of circular and linear M13mp18 ssDNA

Fig. S8 shows data on FnoCas12a RNA-dependent *cis*-cleavage of circular and linear M13 ssDNA. For linearizing M13 circular ssDNA, we used EcoRI restriction enzyme in NEB buffer 2.1. The reaction details are in section 2.7 of the main text. It should be noted that the high-fidelity EcoRI and the Cutsmart buffer composition significantly impaired ssDNA cleavage by this enzyme and that the use of the EcoRI version that is not engineered to have high fidelity was crucial to obtain the observed linearization amounts.

Using data presented in Figs. 2, 4, 7 and S8, one can rank the preferred DNA substrates for FnoCas12a. For FnoCas12a^{WT}, it is ds supercoiled substrate > oligo dsDNA = linearized dsDNA > supercoiled ssDNA plasmid > linearized ssDNA. For FnoCas12a^{KD2P}, it is ds supercoiled substrate > oligo dsDNA > linearized dsDNA > supercoiled ssDNA plasmid > linearized ssDNA. To rank dsDNA oligo, we used the cleavage rate of NTS, since this strand is cut first. The further reduction in TS cleavage for both proteins may relate to impairment of conformational changes essential for coordinated strand cleavages rather than preference of the DNA substrate type. We have not calculated rates for ssDNA cleavage due to the severe deficiencies in cleaving these substrates. Instead, the amount of substrate that was remaining for M13 ssDNA was compared to what was left over for other DNA substrates.

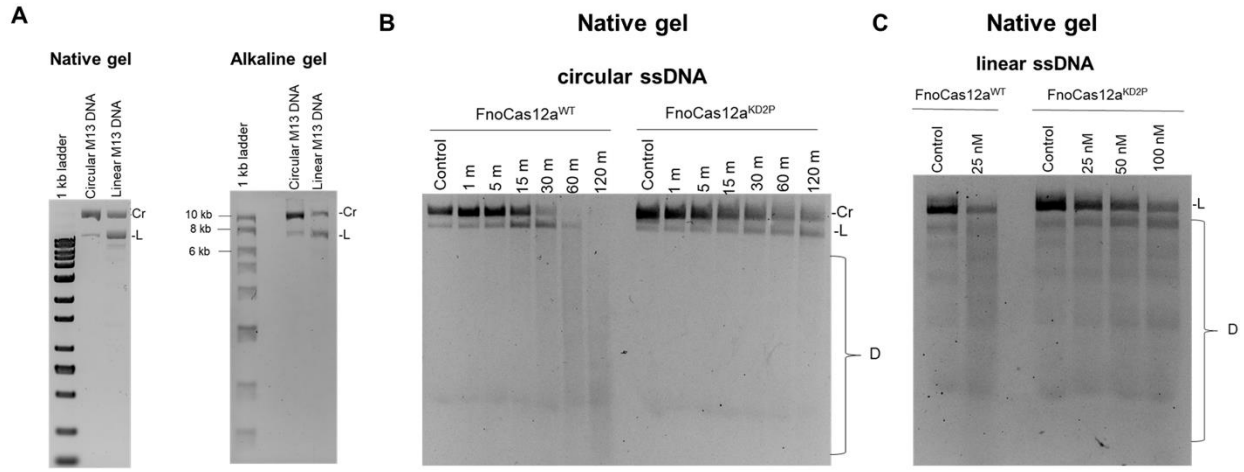

Fig. S8. Analysis of *cis*-cleavage of circular and linear M13mp18 ssDNA (A) Gels showing the efficiency of linearization of M13 ssDNA on a native (left) and an alkaline (right) gel. The alkaline gel, which can give molecular weight corresponding to ssDNA shows a linearized M13 ssDNA at 7 kilobases (kb) and the uncut circular M13 above the linear band. Our preparations gave 50-70% linearization of M13 circular ssDNA with EcoRI. **(B)** Gel showing the *cis*-cleavage of circular M13 ssDNA by FnoCas12a^{WT} and FnoCas12a^{KD2P}. At 25 nM RNP, FnoCas12a^{WT} completely degrades M13 DNA by a combinational effect of *cis*- and *trans*- activities, while FnoCas12a^{KD2P} shows reduced cleavge abilities even after 2 hours. **(C)** Efficiency of *cis*-cleavage by FnoCas12a on linear M13 ssDNA. FnoCas12a^{WT} degraded the linear M13 ssDNA with a moderate efficiency compared to that of FnoCas12^{KD2P}, which did not cleave even at the highest concentration tested. Reactions with linear M13 ssDNA were for 60 min. Representative gels from two replications. [Cr: circular, L: linear, D: degradation, m: min].

Fig. S9. Constructs used to test *trans*-cleavage of ss oligonucleotide DNA. (A) DNA and RNA components for ssDNA activator mediated *trans*-cleavage of ss oligo DNA. The PAM less 20-nt ss activator is completely complementary to the guide region of crRNA. **(B)** DNA and RNA components for dsDNA activator-mediated *trans*-cleavage of ss oligo DNA. The 24-nt dsDNA activator has a region complementary to the crRNA guide along with a PAM (underlined). The ssDNA 20-nt activator and the dsDNA 24-nt activator indicated here were also used for M13 ssDNA *trans* cleavage assay. The ss oligo DNA substrate used for *trans*-cleavage did not possess complementarity with either crRNA or activator DNAs.

Table S1:

Primers used	**Construct**
FnoCas12a^{WT} is used from a previous study (1) NCBI Reference Sequence: WP_003040289.1	FnoCas12a in pET28m [His8-3C-His6-MBP-TEV- FnoCas12a]
FnoCas12a^{KD2P}-FP: 5′TTCAGCTAGG**CCACCC**TGGAAAAAGATAAATAACATCAAAG 3′ FnoCas12a^{KD2P}-RP: 5′ TCCCTATCTTTCTCTATTG 3′	FnoCas12a^{KD2P} in pET28m [His8-3C-His6-MBP-TEV-FnoCas12a]
FnoCas12a-DNA-matched-FP: 5′ gatccTTTAGAGAAGTCATTTAATAAGGCCACTGTTAAAAg 3′ FnoCas12a-DNA-matched-RP: 5′ aattcTTTTAACAGTGGCCTTATTAAATGACTTCTCTAAAg 3′	Matched DNA plasmid in pUC19
FnoCas12a-MM1-FP: 5′ CTAGAggatccTTTA**T**AGAAGTCATTTAATAA 3′ FnoCas12a-MM1-RP: 5′ TTATTAAATGACTTCT**A**TAAAggatccTCTAG 3′	Mismatched DNA position 1 (MM1) in pUC19
FnoCas12a-MM2-FP: 5′CTAGAggatccTTTAG**C**GAAGTCATTTAATAA 3′ FnoCas12a-MM2-RP: 5′ TTATTAAATGACTTC**G**CTAAAggatccTCTAG 3′	Mismatched DNA position 2 (MM2) in pUC19
FnoCas12a-MM3-FP: 5′AGAggatccTTTAGA**T**AAGTCATTTAATAAG 3′ FnoCas12a-MM3-RP: 5′CTTATTAAATGACTT**A**TCTAAAggatccTCT 3′	Mismatched DNA position 3 (MM3) in pUC19
FnoCas12a-MM4-FP: 5′AGAggatccTTTAGAG**C**AGTCATTTAATAAG 3′ FnoCas12a-MM4-RP: 5′CTTATTAAATGACT**G**CTCTAAAggatccTCT 3′	Mismatched DNA position 4 (MM4) in pUC19
FnoCas12a-MM5-FP: 5′AggatccTTTAGAGA**C**GTCATTTAATAAGGC 3′ FnoCas12a-MM5-RP: 5′GCCTTATTAAATGAC**G**TCTCTAAAggatccT 3′	Mismatched DNA position 5 (MM5) in pUC19
FnoCas12a-MM6-FP: 5′AggatccTTTAGAGAA**T**TCATTTAATAAGGC 3′ FnoCas12a-MM6-RP: 5′GCCTTATTAAATGA**A**TTCTCTAAAggatccT 3′	Mismatched DNA position 6 (MM6) in pUC19

FnoCas12a-MM7-FP: 5′AggatccTTTAGAGAAGGCATTTAATAAGGC 3′ FnoCas12a-MM7-RP: 5′GCCTTATTAAATGCCTTCTCTAAAggatccT 3′	Mismatched DNA position 7 (MM7) in pUC19
FnoCas12a-MM8- FP: 5′gatccTTTAGAGAAGTAATTTAATAAGGCCAC 3′ FnoCas12a-MP8- RP: 5′GTGGCCTTATTAAATTACTTCTCTAAAggatc 3′	Mismatched DNA position 8 (MM8) in pUC19
FnoCas12a-MM9-FP: 5′atccTTTAGAGAAGTCCTTTAATAAGGCCAC 3′ FnoCas12a-MM9-RP: 5′GTGGCCTTATTAAAGGACTTCTCTAAAggat 3′	Mismatched DNA position 9 (MM9) in pUC19
FnoCas12a-MM10- FP: 5′cTTTAGAGAAGTCAGTTAATAAGGCCACTGT 3′ FnoCas12a-MP10- RP: 5′ACAGTGGCCTTATTAACTGACTTCTCTAAAg 3′	Mismatched DNA position 10 (MM10) in pUC19
FnoCas12a-MM11-FP: 5′cTTTAGAGAAGTCATGTAATAAGGCCACTGT 3′ FnoCas12a-MM11-RP: 5′ACAGTGGCCTTATTACATGACTTCTCTAAAg 3′	Mismatched DNA position 11 (MM11) in pUC19
FnoCas12a MM12-FP: 5′cTTTAGAGAAGTCATTGAATAAGGCCACTGT 3′ FnoCas12a-MM12-RP: 5′ACAGTGGCCTTATTCAATGACTTCTCTAAAg 3′	Mismatched DNA position 12 (MM12) in pUC19
FnoCas12a-MM13-FP: 5′TTAGAGAAGTCATTTCATAAGGCCACTGTTA 3′ FnoCas12a-MM13-RP: 5′TAACAGTGGCCTTATGAAATGACTTCTCTAA 3′	Mismatched DNA position 13 (MM13) in pUC19
FnoCas12a-MM14-FP: 5′TTAGAGAAGTCATTTACTAAGGCCACTGTTA 3′ FnoCas12a-MM14-RP: 5′TAACAGTGGCCTTAGTAAATGACTTCTCTAA 3′	Mismatched DNA position 14 (MM14) in pUC19
FnoCas12a-MM15-FP: 5′TTAGAGAAGTCATTTAAGAAGGCCACTGTTAAAAg 3′ FnoCas12a-MM15-RP: 5′cTTTTAACAGTGGCCTTCTTAAATGACTTCTCTAA 3′	Mismatched DNA position 15 (MM15) in pUC19
FnoCas12a-MM16-FP: 5′TTAGAGAAGTCATTTAATCAGGCCACTGTTAAAAg 3′ FnoCas12a-MM16-RP: 5′cTTTTAACAGTGGCCTGATTAAATGACTTCTCTAA 3′	Mismatched DNA position 16 (MM16) in pUC19

FnoCas12a-MM17-FP: 5′GAGAAGTCATTTAATA**C**GGCCACTGTTAAAAg 3′ FnoCas12a-MM17-RP: 5′cTTTTAACAGTGGCC**G**TATTAAATGACTTCTC 3′	Mismatched DNA position 17 (MM17) in pUC19
FnoCas12a-MM18-FP: 5′GAGAAGTCATTTAATAA**T**GCCACTGTTAAAAg 3′ FnoCas12a-MM18-RP: 5′cTTTTAACAGTGGC**A**TTATTAAATGACTTCTC 3′	Mismatched DNA position 18 (MM18) in pUC19
FnoCas12a-MM19-FP: 5′AAGTCATTTAATAAG**T**CCACTGTTAAAAgaa 3′ FnoCas12a-MM19-RP: 5′ttcTTTTAACAGTGG**A**CTTATTAAATGACTT 3′	Mismatched DNA position 19 (MM19) in pUC19
FnoCas12a-MM20-FP: 5′AAGTCATTTAATAAGG**A**CACTGTTAAAAgaa 3′ FnoCas12a-MM20-RP: 5′ttcTTTTAACAGTG**T**CCTTATTAAATGACTT 3′	Mismatched DNA position 20 (MM20) in pUC19
FnoCas12a-MM21-FP: 5′GTCATTTAATAAGGC**A**ACTGTTAAAAgaatt 3′ FnoCas12a-MM21-RP: 5′aattcTTTTAACAGT**T**GCCTTATTAAATGAC 3′	Mismatched DNA position 21 (MM21) in pUC19
FnoCas12a-MM22-FP: 5′GTCATTTAATAAGGCC**C**CTGTTAAAAgaatt 3′ FnoCas12a-MM22-RP: 5′aattcTTTTAACAG**G**GGCCTTATTAAATGAC 3′	Mismatched DNA position 22 (MM22) in pUC19

Table S1: Primers used in this study. The table includes the various primers used for cloning FnoCas12a^{KD2P}. The DNA sequence coding for proline substitution is in bold. The primers used to create substrate plasmids are shown. The PAM region is underlined, nucleotide mismatch position is shown in red and restriction enzyme sites used for cloning are shown in small letters.

Table S2:

DNA oligos	Purpose
crRNA-template strand for matched plasmid and oligo assays: 5′AGTGGCCTTATTAAATGACTTCTCATCTACAACAG TAGAAATTCCC*TATAGTGAGTCGTATTA*ATTTC 3′ T7 promoter top strand: 5′GAAAT*TAATACGACTCACTATA*GGG3′	FnoCas12a- matched DNA crRNA transcription oligos [Protocol adapted from (2)]
crRNA-template strand for M13 mp18 ssDNA *cis*-cleavage assays: 5′GCGGATAACAATTTCACACAGATCTACAACAGTAG AAATTCCC*TATAGTGAGTCGTATTA*ATTTC 3′ T7 promoter top strand: 5′GAAAT*TAATACGACTCACTATA*GGG3′	FnoCas12a- M13 crRNA transcription oligos [Protocol adapted from (2)]
5′GCGGATAACAATTTCACACAGGAAA 3′	Protospacer sequence in M13 ssDNA
5′ GCCTTATTAAATGACTTCTC 3′	ssDNA (20-nt) activator
TS: 5′ GCCTTATTAAATGACTTCTCTAAA 3′ NTS: 5′ TTTAGAGAAGTCATTTAATAAGGC 3′	dsDNA (24-nt) activator
TS: 5′ GTCAATTCTTTTAACAGTGGCCTTAT TAAATGACTTCTCTAAAGGATCAT 3′ NTS: 5′ ATGATCCTTTAGAGAAGTCATTTAATA AGGCCACTGTTAAAAGAATTGAC 3′	Matched dsDNA oligo for cleavage assay and EMSA.
TS: 5′ GTCAATTCTTTTAACAGTGGCCTTAT TAAAT**T**ACTTCTCTAAAGGATCAT 3′ NTS: 5′ ATGATCCTTTAGAGAAGT**A**ATTTAATA AGGCCACTGTTAAAAGAATTGAC-3′	MM8 dsDNA oligo with mismatch at position 8 for cleavage assay and EMSA.
17 nt marker: 5′ GTCAATTCTTTTAACAG 3′ 29 nt marker: 5′ ATGATCCTTTAGAGAAGTCATTTAATAAG 3′	ssDNA ladder for oligo cleavage products
5′ CGACGGCCAGTGAATTCCCCAAAAAGCGC AAGAAGAAATCAACCAGCGCAGGAT 3′	ssDNA substrate for *trans*-cleavage

5′AGCAGATTGTACTGAGAGTGCACCATATGCGGTGTGAAATACCGCACAGATGCGTAAGGA 3′	ssDNA substrate for RNA-independent DNA cleavage

Table S2: DNA substrates used in this study. This table includes the DNA templates for *in vitro* transcription of crRNAs, oligo cleavage substrates (both *cis*- and *trans*-), activators for *trans*-cleavage and DNA ladders used in study. T7 promoter region is italicized, PAM is underlined, and mismatches are in red.

Table S3

BH amino acid	Interacting partner	Distance (Å)	Type of interaction
Y953	**I944 of RuvC-I motif**	**4.0**	**Hydrophobic**
	T951 of RuvC-I motif	**3.7**	**Hydrophobic**
	Y984 of RuvC-II motif	**3.3**	**Hydrophobic**
	A(-11) of pseudoknot	**3.8**	**Hydrogen bond**
H954	N942 **of RuvC-I motif**	4.4	Hydrophobic
K956	**C(-10) of pseudoknot**	**2.6**	**Ionic through phosphate**
	A(-11) of pseudoknot	**2.9**	**Ionic through sugar**
L957	L923 of RuvC-I motif	4.2	Hydrophobic
	K981 of RuvC-II motif	**3.3**	**Hydrophobic**
I960	**M980 of RuvC-II motif**	**3.6**	**Hydrophobic**
	I977 of RuvC-II motif	**3.0**	**Hydrophobic**
E961	V1019 of RuvC-II motif	4.4	Hydrophobic
D963	**K972 of RuvC-II motif**	**3.7**	**Ionic**
R964	I974 & I977 of RuvC-II motif	4.2 & 4.2	Hydrophobic
R968	**G11 of guide**	**3.0**	**Ionic through sugar**
	U12 of guide	**3.2**	**Ionic through sugar**
K969	**A13 of guide**	**4.0**	**Ionic through phosphate**
	K527 of REC2 motif	**2.8**	**Hydrogen bond**
D970	**K524 of REC2 motif**	**3.8**	**Ionic**
W971	**R583 of REC2 motif**	**3.6**	**Hydrophobic**
	Y579 of REC2 motif	**3.7**	**Hydrophobic**
	L530 of REC2 motif	4.1	Hydrophobic
	I582 of REC2 motif	4.1	Hydrophobic
	V523 of REC2 motif	4.5	Hydrophobic
	I586 of REC2 motif	4.4	Hydrophobic
	T587 of REC2 motif	4.2	Hydrophobic

Table S3: List of interactions of FnoCas12a BH with crRNA and different protein domains. The BH has several interactions with the REC2 domain, RuvC-I and II motifs and crRNA. The interactions in bold are all within the 2-4 Å range. The list shows the type of molecule (protein/RNA/DNA), type of interaction, as well as the distance for each interaction. Although W971 is not part of the BH, we included it on the list since it is the first amino acid after BH and has multiple interactions with the REC2 domain. The interaction details were prepared using PyMol and Arpeggio (3,4).

Table S4:

Type of substrate	Rate constants for FnoCas12a^{WT} (min^{-1})	Fold change for FnoCas12a^{WT} compared to supercoiled dsDNA	Rate constants for FnoCas12a^{KD2P} (min^{-1})	Fold change for FnoCas12a^{KD2P} compared to supercoiled dsDNA	Fold change FnoCas12a^{WT}/ FnoCas12a^{KD2P} for each substrate
Supercoiled dsDNA	k1 =12.7 ±3.2 k2 =0.08 ±0.04	**NA**	k1 =4.17 ± 0.42 k2 =0.14 ± 0.05	**NA**	3
Oligo dsDNA (TS)	k_{obs} = 2.03 ± 0.14	6	k_{obs} = 0.34 ± 0.08	12	6
Oligo dsDNA (NTS)	k_{obs} = 2.90± 0.36	4	k_{obs} = 1.13± 0.18	4	3
Linearized plasmid dsDNA	k_{obs} = 3.12± 0.24	4	k_{obs} = 0.35 ± 0.03	12	9

Table S4: The compilation of the rate constants calculated for different physical states of dsDNA substrates in the study and respective fold changes for FnoCas12a^{WT} and FnoCas12a^{KD2P}. In the column adjacent to the individual rates for each protein, we have included the fold change of rates relative to that of the supercoiled dsDNA substrate (k1), since it was the most preferred among all the DNA substrates that we tested. The last column has respective fold changes for each substrate type between FnoCas12a^{WT} and FnoCas12a^{KD2P}. [NA: Not applicable].

Table S5:

Amino acid	Interacting partner
K341 of REC2	dC (-11) of TS
D396 of REC2	C17 of crRNA guide
T400 of REC2	dA (-20) of TS
Q404 of REC2	dA (-20) and dC -21 of TS
D408 of REC2	dC (24) of NTS
Y410 of REC2	dA (-20) of TS
N534 of REC2	U (15) and A (14) of crRNA guide
H538 of REC2	interacts with Water 1503, which in turn interacts with U (16), U (15) of crRNA guide
K541 of REC2	interacts with Water 1503, which in turns interacts with U (16) of crRNA guide
V576 of REC2	U (15) and A (14) of crRNA guide
Y579 of REC2	A (13) and A (14) of crRNA guide and W971 of RuvC-II motif
N580 of REC2	A (14) of crRNA guide
R583 of REC2	A (14) and A (13) of crRNA guide, dA (-12) of TS and W971 of RuvC-II motif
N584 of REC2	dC (-11) and dA (-12) of TS
I586 of REC2	W971 and K972 of RuvC-II motif
T587 of REC2	dC (-11) and dC (-10) of TS and W971 of RuvC-II motif
Q588 of REC2	dC (-11) and dC (-10) of TS and K972 of RuvC-II motif
K589 of REC2	dC (-10), dT (-9) and dC (-11) of TS
K978 of RuvC-II	dT (-8) of TS

Table S5: List of interactions of crRNA and DNA with REC2 and RuvC domains (only interactions closer to the mismatch positions shown). All DNA bases are denoted by a "d" ahead of the nucleotide base. For TS DNA, a negative sign (for example, dA (-base number)) refers to bases in the protospacer region after the PAM. A positive number refers to protospacer region after the PAM in the case of NTS DNA. The interaction details were prepared using PyMol and Arpeggio (3,4).

References

1. Sundaresan, R., Parameshwaran, H. P., Yogesha, S. D., Keilbarth, M. W., and Rajan, R. (2017) RNA-Independent DNA Cleavage Activities of Cas9 and Cas12a. *Cell Rep.* **21**, 3728-3739
2. Zetsche, B., Gootenberg, J. S., Abudayyeh, O. O., Slaymaker, I. M., Makarova, K. S., Essletzbichler, P., Volz, S. E., Joung, J., van der Oost, J., Regev, A., Koonin, E. V., and Zhang, F. (2015) Cpf1 is a single RNA-guided endonuclease of a class 2 CRISPR-Cas system. *Cell* **163**, 759-771
3. DeLano, W. L. (2002) Pymol: An open-source molecular graphics tool. *CCP4 Newsletter On Protein Crystallography*, 82-92
4. Jubb, H. C., Higueruelo, A. P., Ochoa-Montaño, B., Pitt, W. R., Ascher, D. B., and Blundell, T. L. (2017) Arpeggio: A Web Server for Calculating and Visualising Interatomic Interactions in Protein Structures. *J Mol Biol* **429**, 365-371